BOREAL ENVIRONMENT RESEARCH 14: 559–575
ISSN 1239-6095 (print) ISSN 1797-2469 (online)

Helsinki 31 August 2009

Ion-UHMA: a model for simulating the dynamics of neutral and charged aerosol particles

Johannes Leppä[1)], Veli-Matti Kerminen[1)], Lauri Laakso[2)3)], Hannele Korhonen[4)], Kari E. J. Lehtinen[4)5)], Stéphanie Gagné[2)], Hanna E. Manninen[2)], Tuomo Nieminen[2)] and Markku Kulmala[2)]

[1)] *Finnish Meteorological Institute, Climate Change, P.O. Box 503, FI-00101 Helsinki, Finland*
[2)] *Department of Physics, P.O. Box 64, FI-00014 University of Helsinki, Finland*
[3)] *School of Physical and Chemical Sciences, North-West University, Private Bag x6001, Potchefstroom 2520, Republic of South Africa*
[4)] *Department of Physics, University of Kuopio, P.O. Box 1624, FI-70811 Kuopio, Finland*
[5)] *Finnish Meteorological Institute, Kuopio Unit, P.O. Box 1624, FI-70811 Kuopio, Finland*

Received 19.Dec. 2008, accepted 13 Mar. 2009 (Editor in charge of this article: Jaana Bäck)

Leppä, J., Kerminen, V.-M., Laakso, L., Korhonen, H., Lehtinen, K. E. J., Gagné, S., Manninen, H. E., Nieminen, T. & Kulmala, M. 2009: Ion-UHMA: a model for simulating the dynamics of neutral and charged aerosol particles. *Boreal Env. Res.* 14: 559–575.

A new aerosol dynamical box model, Ion-UHMA (University of Helsinki Multicomponent Aerosol model for neutral and charged particles), is introduced in this paper. The model includes basic dynamical processes (condensation, coagulation and deposition) as well as ion–aerosol attachment and ion–ion recombination. The formation of particles is treated as model input or, alternatively, the model can be coupled with an existing nucleation model. Ion-UHMA was found to be able to reproduce qualitatively the measured time evolution of the particle number size distribution, when the particle formation and growth rates as well as concentrations of particles > 20 nm in diameter were taken from measurements. The simulated charging state of freshly formed particles during a new particle formation event evolved towards charge equilibrium in line with previously-derived analytical formulae. We provided a few illustrative examples to demonstrate possible applications, to which the Ion-UHMA model could be used in the near future.

Introduction

The formation of new atmospheric aerosol particles by nucleation and subsequent growth has been found to take place in a variety of environments ranging from clean polar areas to polluted urban centers (*see* Kulmala *et al*. 2004b, Kulmala and Kerminen 2008, and references therein). Atmospheric aerosol formation is able to maintain a substantial background aerosol particle population over boreal forests during the spring to autumn period (Tunved *et al*. 2006, Dal Maso *et al*. 2007). It may give a significant contribution to the global budget of the total particle number concentration (Spracklen *et al*. 2006). After their growth to larger sizes, aerosol particles formed originally in the atmosphere may become cloud condensation nuclei and participate to cloud droplet activation (e.g. Kerminen *et al*. 2005, Laaksonen *et al*. 2005, Pierce and

Adams 2007, 2009, Spracklen *et al*. 2008, Makkonen *et al*. 2009, Wang and Penner 2009).

Several atmospheric nucleation pathways have been proposed, including homogeneous binary or ternary nucleation of different vapors, kinetic nucleation (Weber *et al*. 1996, Kuang *et al*. 2008) and heterogeneous nucleation (activation) on pre-existing molecular clusters (Hoppel *et al*. 1994, Kulmala *et al*. 2006, Sihto *et al*. 2006, Riipinen *et al*. 2007). Both binary and ternary homogeneous nucleation can proceed via neutral pathways or they can be assisted by the presence of ions, the latter being usually termed as ion-induced or ion-mediated nucleation (e.g. Yu *et al*. 2006). Ions may also contribute to neutral nucleation by producing neutral clusters via ion-ion recombination (Arnold 1980). When molecular clusters are present, as one might expect under many atmospheric conditions (e.g. Kulmala *et al*. 2007), heterogeneous nucleation is preferred over homogeneous one and charged clusters tend to be activated before neutral clusters (Winkler *et al*. 2008). As a result, several nucleation mechanisms may be operating in parallel or over the course of the day, as indicated by recent measurements by Laakso *et al*. (2007b).

In order to quantify the regional and global effects resulting from atmospheric aerosol formation, we should have better understanding of the initial steps of this phenomenon in different atmospheric environments (e.g. Kulmala *et al*. 2004c). Continuous field measurements play a key role in this regard. Unfortunately, the great majority of the conducted measurements are not suitable for investigating the very early steps of aerosol formation, since the used instruments do not usually measure particles smaller than a few nanometers in diameter. In this study, diameter always refers to Millikan (mobility equivalent) diameter.

Air ion spectrometers provide means to measure the number distributions of charged particles and ion clusters down to molecular sizes (Tammet 2006, Mirme *et al*. 2007, Asmi *et al*. 2009). Various kinds of air ion spectrometers have been applied in a number of short- and long-term field studies and a lot of new insight into atmospheric aerosol formation has been obtained (e.g. Hõrrak *et al*. 2003, Vana *et al*. 2004, Hirsikko *et al*. 2005, Iida *et al*. 2006, Kulmala and Tammet 2007, Siingh *et al*. 2007, Vartiainen *et al*. 2007, Junninen *et al*. 2008, Suni *et al*. 2008). Another type of instrument measuring both neutral and charged particles down to about 3 nm is the ion-Differential Mobility Particle Sizer (ion-DMPS; Laakso *et al*. 2007a). The ion-DMPS has been designed specifically to investigate the relative role of neutral and ion-induced particle formation pathways (Kerminen *et al*. 2007, Laakso *et al*. 2007a, Gagné *et al*. 2008).

Getting the full advantage of current air ion spectrometer and ion-DMPS measurements may not be possible without the help of a dynamical model that is able to capture the basic interactions between ion clusters, charged and neutral particles, and condensing vapors. Here we will introduce a new dynamical box model for this purpose, called Ion-UHMA. The new model builds on the aerosol dynamical model UHMA (Korhonen *et al*. 2004) and the AEROION model (Laakso *et al*. 2002). It should be noted that a number of detailed models simulating the dynamics of molecular-size clusters have already been developed (Yu and Turco 2001, Laakso *et al*. 2002, Kazil and Lovejoy 2004, Lovejoy *et al*. 2004, Sorokin *et al*. 2006, Yu 2006). While extremely useful in studying ion-induced nucleation, these models simulate only clusters containing sulfuric acid, water and their ion derivatives. The Ion-UHMA does not aim to simulate the actual nucleation process but takes the formation rates of neutral and charged particles as a model input. This way, the Ion-UHMA is not restricted to any particular nucleation mechanism or specific chemical compounds. In addition to describing and testing the Ion-UHMA, we will present a few examples on its potential application to investigate atmospheric aerosol formation events.

Model description

Ion-UHMA is a zero-dimensional sectional box model, which simulates the dynamics of neutral and electrically charged aerosol particles in atmospheric conditions. The emphasis of the model is on the difference between dynamics of neutral and charged nanometer-sized particles.

Size and charge distribution description

The model is a zero-dimensional sectional box model. The upper and lower limits of the simulated particle diameter range are specified by the user. The particles in the model are divided into user specified number of size sections and every size section is divided into three charge classes: neutral, negative and positive. Particles with multiple charges are treated the same way as the particles with one elementary charge. This causes very small errors for particles smaller than 20 nm in diameter and additional charge classes would make the model computationally too heavy. The fractions of negative and positive particles in the initial size distribution are treated as input parameters, with the same value for all size sections.

The sectional method used is the fixed hybrid method (Jacobson and Turco 1995), in which the particles are divided into sections of fixed size according to the volume of their core compounds. The radii of particles are then determined by calculating the amount of noncore compounds, in our case assuming that the particles reach equilibrium with ambient ammonia and water. In case of particles being formed smaller than the smallest size section or growing beyond the largest size section, the particles are put into the nearest size sections conserving the particle volume concentration and under- or overestimating the particle number concentration.

The problem with the fixed sections is the numerical diffusion; the artificial broadening of the distribution as the particles falling between two sections are divided into those two sections according to their core volumes. The hybrid method is capable of treating the relevant dynamical processes, if big enough number of size sections is used.

Besides the particle distribution described above, the model includes pools for negatively and positively charged clusters. The clusters represent particles with diameter smaller than ~2 nm, which are constantly observed in the charged particle measurements. These clusters are allowed to attach to particles and to recombine with each other. The production rate of clusters is treated as an input parameter. The formation of new particles may be set to act as a sink for charged clusters, if desired. The cluster mass, radius and mobility are input parameters, with different values for each charge class.

Particle composition

The particles in the model are divided into the size sections based on the volume of their core. The core compounds are sulfuric acid, water-soluble organic compounds and an arbitrary number of insoluble compounds. The insoluble compounds describe insoluble organic matter, mineral dust and black carbon, and they are not allowed to condense to or evaporate from the particles. The water and ammonia contents are not included in the core of the particles, but their amount in the particles is calculated assuming that the particles are in equilibrium with ambient ammonia and water (Napari *et al*. 2002).

The chemical composition of particles is traced individually for each size and charge section, but all the particles in one section have the same composition. It is possible to have particles that have the same size but different composition in the model, if the composition is different in different charge classes of one size section.

Aerosol microphysics

The dynamic equations governing the particle number concentrations in section i may be written as:

$$\begin{aligned}
\frac{dN_i^0}{dt} &= P_i^0 - V_{\mathrm{d},i} N_i^0 \\
&+ \frac{1}{2}\sum_{k=1}^{z}\sum_{l=1}^{z} \chi_{kli} N_k^0 N_l^0 K_{kl}^{00} \\
&+ \sum_{k=1}^{z}\sum_{l=1}^{z} \chi_{kli} N_k^+ N_l^- K_{kl}^{+-} \\
&- \sum_{j=1}^{z} N_i^0 N_j^0 K_{ij}^{00} - \sum_{j=1}^{z} N_i^0 N_j^{\pm} K_{ij}^{0\pm} \\
&- \frac{\sum_{m=1}^{y} \delta V_{m,i}^0 N_i^0}{V_{i+1} - V_i} + \frac{\sum_{m=1}^{y} \delta V_{m,i-1}^0 N_{i-1}^0}{V_i - V_{i-1}} \\
&- N_i^0 N_{\mathrm{C}}^{\pm} \beta_0 \left(d_{\mathrm{p},i}^0 \right) + \mathrm{Attach}_i^0
\end{aligned} \tag{1}$$

$$\begin{aligned}\frac{dN_i^{\pm}}{dt} &= P_i^{\pm} - V_{\mathrm{d},i}N_i^{\pm} \\ &+\frac{1}{2}\sum_{k=1}^{z}\sum_{l=1}^{z}\chi_{kli}N_k^{\pm}N_l^{\pm}K_{kl}^{\pm\pm} \\ &+\sum_{k=1}^{z}\sum_{l=1}^{z}\chi_{kli}N_k^{\pm}N_l^{0}K_{kl}^{\pm 0} \\ &-\sum_{j=1}^{z}N_i^{\pm}N_j^{\pm}K_{ij}^{\pm\pm} \\ &-\sum_{j=1}^{z}N_i^{\pm}N_j^{\mp}K_{ij}^{\pm\mp} - \sum_{j=1}^{z}N_i^{\pm}N_j^{0}K_{ij}^{\pm 0} \\ &-\frac{\sum_{m=1}^{y}\delta V_{m,i}^{\pm}N_i^{\pm}}{V_{i+1}-V_i} + \frac{\sum_{m=1}^{y}\delta V_{m,i-1}^{\pm}N_{i-1}^{\pm}}{V_i - V_{i-1}} \\ &-N_i^{\pm}N_{\mathrm{C}}^{\pm}\beta_1\left(d_{\mathrm{p},i}^{\pm}\right) - N_i^{\pm}N_{\mathrm{C}}^{\mp}\beta_{-1}\left(d_{\mathrm{p},i}^{\pm}\right) \\ &+\mathrm{Attach}_i^{\pm}\end{aligned} \tag{2}$$

in which

$$\chi_{kli} = \begin{cases} \dfrac{V_{i+1}-\left(V_k+V_l\right)}{V_{i+1}-V_i}; & \text{if } V_i \le V_k+V_l < V_{i+1} \\ \dfrac{\left(V_k+V_l\right)-V_{i-1}}{V_i-V_{i-1}}; & \text{if } V_{i-1} < V_k+V_l < V_i. \\ 0; & \text{otherwise} \end{cases} \tag{3}$$

Here N is the particle number concentration, N_{C} is the concentration of charged clusters, V is the volume of the core compounds in the particle, δV_m is the change rate of the volume of the core compounds in the particle due to condensation or evaporation of the compound m, P is the particle production rate, V_{d} is the deposition velocity, K is the coagulation coefficient, β_{-1} is the recombination coefficient of charged cluster and oppositely charged particle, β_0 and β_1 are the attachment coefficients of a charged cluster and neutral or similarly-charged particle, respectively, and d_{p} is the particle diameter. The upper (0, + and –) and lower indices (i, j, k and l) represent the charge class and size section of the particles respectively, and z and y are the number of size sections and condensable compounds in the simulation, respectively. In the condensation/evaporation terms given here it is assumed that condensation dominates over evaporation. The last terms in Eqs. 1 and 2 represent the particles put into the section as a result of attachment and/or recombination of a charged cluster and a particle. Equations 1 and 2 are solved in the model using the Euler forward method. When the particle number concentration of a section is changed according to Eq. 1 or 2, the corresponding volume concentrations of core compounds are changed accordingly.

Particle formation

The Ion-UHMA model does not aim to simulate the actual nucleation process. Instead, our approach is to take as model inputs the formation rates of neutral and charged particles at sizes (around 1.5–2 nm) where these particles are ready to grow by vapor condensation. This way, simulated particles can be thought to be nucleated thermodynamically or kinetically via neutral or ion-induced pathways, and the particle growth may either follow directly the nucleation process or start from the "activation" of charged or neutral clusters (Kulmala *et al*. 2006).

Condensation

Condensation of vapor molecules on the particle surfaces is the most important process behind the observed growth of aerosol particles in the atmosphere. Conventionally, the flux of molecules onto the particle surface is calculated assuming that the diffusion coefficient of the particle is negligible compared to that of vapor molecule. The assumption becomes less valid as the particles get smaller and eventually close to molecular sizes. In the Ion-UHMA the non-continuum effects in the collision rates are corrected using the formulation by Fuchs and Sutugin (1971), which is furthermore corrected according to Lehtinen and Kulmala (2003), to take into account the molecule-like properties of nanometer-sized particles. The collision frequency of the molecules to charged particles is enhanced due to particle charging. In Ion-UHMA, this is taken into account using the equation (Lushnikov and Kulmala 2004)

$$\xi\left(d_{\mathrm{p}}\right) = 1 + \frac{\gamma e^2 r}{d_{\mathrm{p}}^2}, \tag{4}$$

where ξ is the correction to the collision frequency, d_{p} is the particle diameter, e is the elementary charge, $\gamma = 1/kT$, were T is the

temperature in Kelvin degrees and k is the Boltzmann constant. A polar molecule can formally be described as a compound having a negative and positive charge set a part by a fixed distance. This distance is denoted by r in Eq. 4.

The above formulation of collision frequency leaves the mass accommodation coefficient of vapor molecules on particle surfaces as an input parameter. While some experimental studies suggest that the accommodation coefficient could be significantly smaller than one for many compounds (Worsnop *et al*. 2001, Guimbaud *et al*. 2002, Davidovits *et al*. 2006), others report values close to unity (Hanson and Kosciuch 2003, Winkler *et al*. 2004, Voigtländer *et al*. 2007), which is furthermore supported by theoretical studies (Clement *et al*. 1996, Kulmala and Wagner 2001, Morita 2003). In our model, the value of the mass accommodation may be chosen individually for each compound, the default value being equal to 1 for all compounds.

The very low saturation vapor pressure of sulfuric acid makes it eager to condense onto particles. Usually only a small fraction of observed particle growth rate is caused by sulfuric acid, but the very low volatility makes it a possibly important component of the growth of particles with diameter of few nanometers (*see* e.g. Fiedler *et al*. 2005). In Ion-UHMA, sulfuric acid is assumed to be nonvolatile.

One of the main problems in describing atmospheric condensation is the huge variety of low or semi volatile organic vapors and poor knowledge of their properties. Experimental studies suggest that growth of the particles is mostly due to organic vapors, at least in forested areas (O'Dowd *et al*. 2002, Allan *et al*. 2006, Smith *et al*. 2008), but detecting actual species is very difficult. For the sake of simplicity, the organic vapors in Ion-UHMA are described by only a few compounds. The number and properties of these compounds are set by the user depending on the work at hand. The properties used to describe the organic vapors are density, molar mass, surface tension, diffusion volume, saturation vapor pressure over flat surface, mass accommodation coefficient and hygroscopic growth factor. The saturation vapor pressure over the particle surface is calculated either by using the Kelvin equation or by using the nano-Köhler theory (Anttila *et al*. 2004). The former takes into account only the curvature of the particle and surface tension of the condensing compound, while the latter also takes into account the composition of the particle.

Coagulation

Coagulation includes three processes in the model: collisions between particles, attachment of cluster-ions to particles and recombination of charged clusters. The coagulation coefficients are calculated at the beginning of the simulation, after which they are recalculated when the value of ambient temperature or relative humidity has been changed by more than 1% or 20%, respectively, or when the radius of particles in any section has changed by more than 1%. The recombination coefficient of clusters in the model is set equal to 1.6×10^{-6} cm^3 s^{-1} (Hoppel and Frick 1990, Tammet and Kulmala 2005).

The coagulation coefficients are calculated using the flux matching theory according to Fuchs (1964). In case of one or both of the particles being charged, the coagulation coefficient is corrected according to Howard *et al*. (1973) and Mick *et al*. (1991). This correction takes into account both the Coulomb and Van der Waals forces.

The attachment coefficient between positive (negative) cluster ion and particle with i ($-i$) elementary charges is calculated using parameterized version (Hõrrak *et al*. 2008) of the theory presented by Hoppel and Frick (1986):

$$\beta_i\left(d_\mathrm{p}\right) = \frac{2\pi d_\mathrm{p} kTZ}{e} \frac{x}{\exp\left(x\right)-1} \times \sqrt{1-\frac{2}{2+i\left(i-1\right)+d_\mathrm{p}/\left(10\ \mathrm{nm}\right)}}, \quad (5)$$

where Z is the mobility of clusters, $x = ie^2/(2\pi d_\mathrm{p}\varepsilon_0 kT)$, ε_0 is the electric constant, e is the elementary charge, k is the Boltzmann constant and T is the temperature.

Dry deposition

In dry deposition, particles are removed from

the carrier gas by collisions to surfaces. In Ion-UHMA, dry deposition is treated using the semi empirical deposition model according to Rannik *et al*. (2003). The model is based on eddy covariance measurements of particle number fluxes and particle size distribution measurements conducted at Hyytiälä forest station in southern Finland. The used flux measurements are limited to particles with diameters from 10 to 500 nm. In the parameterization implemented to Ion-UHMA, the model is extrapolated to sizes below 10 nm while accounting for the size dependence of deposition velocity controlled by the Brownian deposition mechanism.

In theory, the dry deposition is enhanced due to electrical interactions, and the role of electric deposition may be important, if the wind speed is low (Tammet *et al*. 2001). This is not taken into account in the Ion-UHMA model, in which charged particles are treated the same way as neutral particles when calculating the dry deposition.

Model evaluation

Several tests were conducted in order to evaluate the model performance. These tests included comparisons with the well-tested UHMA model, as well as both quantitative and qualitative examination of the dynamics related to charged particles and clusters. If the initial particle distribution is purely neutral, if new particles are formed via neutral nucleation and if the concentration of charged clusters is set to zero at all times, the Ion-UHMA should give the same output as the UHMA model, provided that the inputs are the same for both models. This was the case in all compared simulations, except the ones with coagulation. In those simulations there was a negligible difference due to non-continuous calculation of the coagulation coefficients in the Ion-UHMA where the coefficients are recalculated only if particle radii or ambient temperature and relative humidity change substantially (*see* Coagulation).

The major differences between the dynamics of charged and neutral particles are the potentially enhanced condensation onto charged particles and the differences in coagulation and ion-aerosol attachment rates. The condensation flux into charged particles was greater than the flux into neutral ones according to Eq. 4. The overall effect of enhanced condensation on the particle population was found to be important for particles in the smallest size sections, but very small for particles larger than about 5 nm. Independent of the initial charge distribution, the particle population evolved towards charge equilibrium. This was partly due to coagulation, but mainly due to ion-aerosol attachment. Also the freshly formed particles evolved towards charge equilibrium, a topic which will be covered later in this paper.

Simulations

In this section, we present results from two sets of simulations (sets 1 and 2) and compare the results to measured data. The input parameters for set 1 do not represent any actual new particle formation event, but were chosen to give a possible description of conditions of a new particle formation event day in boreal forest. For set 2, the input parameters were mainly taken from measured data in order to test the model's performance in reproducing the behavior of particle size distribution in the atmosphere and to show possible ways to use the model in future studies.

Time evolution of the aerosol number size distribution during nucleation events

Set 1 included six simulations (cases 1–6), which were conducted using 60 size sections for the diameter range from 1.8 nm to 1.0 μm. The ambient temperature, relative humidity and ammonia mixing ratio were assumed to be equal to 283.15 K, 50%, and 5 ppt, respectively. The initial size distribution was a combination of two lognormal modes (Table 1). The boundary layer height was set to raise from 200 to 600 m between 07:00 and 11:00 and the rise was simulated by diluting the particle concentrations assuming mixing with particle free air. The sulfuric acid concentration had a base level of 1.0×10^5 cm^{-3} and the concentration was set to follow a sinusoidal pattern between 07:00 and 19:00, with a peak

concentration of 7.0×10^6 cm^{-3}. The organic vapor concentration was set to constant value of 2.0×10^7 cm^{-3}. The density, molar mass, surface tension, diffusion volume and hygroscopic growth factor of the organic vapor were set to 1107 kg m^{-3}, 150 g mol^{-1}, 30×10^{-3} N m^{-1}, 51.96 cm^3 and 1.0, respectively. The saturation concentration of the organic vapor over flat surface was chosen to be equal to 1.0×10^6 cm^{-3} and the saturation vapor pressure over the particle surface was calculated according to nano-Köhler theory (Anttila *et al*. 2004, Kulmala *et al*. 2004a). As a result, the organic vapor begun to condense onto particles with a diameter of about 2.4 nm. The enhanced collision frequency of condensing molecules onto charged particles, described by Eq. 4, was taken into account only for sulfuric acid, for which the polarity assumption is valid. The initial ion cluster concentration and formation rate of clusters had values of 500 cm^{-3} and 5 cm^{-3} s^{-1}, respectively, for both charges. The formation rate of particles was set to follow sinusoidal pattern between 08:00 and 16:00, with the highest rate of 2.0 cm^{-3} s^{-1} occurring at noon. At other times, there was no particle production. All particles were produced in the smallest section of corresponding charge class.

In case 1, completely neutral particle formation was assumed. In case 2, 10% of the freshly formed particles were assumed to be negatively charged and 5% positively charged. In case 3, 50% of the particles were assumed to be formed negative and 50% positive. The values were chosen to cover both extreme situations of purely neutral and purely ion-induced nucleation, as well as one case with fraction of ion-induced nucleation in line with predictions by Laakso *et al*. (2007a). The formation of charged particles was set to act as a sink for clusters of corresponding charge.

For cases 1, 2 and 3, a clear new particle formation event was observed for all charges (Figs. 1, 2 and 3). The newly formed mode grew eventually to sizes of some tens of nanometers, with negligible differences seen in the modal growth rate between the different charges. The concentrations of charged particles were smaller than those of neutral particles of the same size. With increasing particle diameter, however, the relative difference between the concentrations decreased. The diameters of charged clusters were smaller than the lower limit of the simulated size range, so the clusters are not shown in Figs. 1–3.

A clear difference between the cases was observed in the smallest sizes. In case 1, charged particles were not clearly observable until around the diameter of 3 nm, the main reason being that the only source of these particles was the charging of originally neutral particles by ion-aerosol attachment. The clear gap between the charged clusters (< 2 nm) and smallest charged particles (~3 nm) is in line with atmospheric measurements, in which a similar gap has frequently been observed (e.g. Hirsikko *et al*. 2007, Komppula *et al*. 2007, Suni *et al*. 2008).

In cases 2 and 3, the population of charged particles included particles formed by ion-induced nucleation as well as particles charged by ion-aerosol attachment. In case 3, concentrations of neutral particles in the smallest size sections were significantly smaller than corresponding concentrations in cases 1 and 2, but the difference decreased with increasing particle size and was not observable after the diameter of about 3 nm. Concentrations of neutral and total particles in the smallest sizes were clearly smaller in case 3 as compared with cases 1 and 2. This can be explained by the combined effect

Table 1. Parameters describing the initial particle size distribution of simulation cases 1–6 in set 1. The distribution comprises two lognormal modes with mean diameters, μ, the total particle concentrations, N_{tot}, and the standard deviations, σ. The particles are composed of sulfuric acid and an organic compound with the same fractions used for each size section. The fraction of negatively and positively charged particles is the same for both polarities and for each size section.

μ (nm)	N_{tot} (cm^{-3})	σ	Fraction of H_2SO_4 (%)	Fraction of organic compound (%)	Charged fraction (%)
20.0	3.5×10^3	1.6	60	40	15
80.0	0.064×10^3	1.3	60	40	15

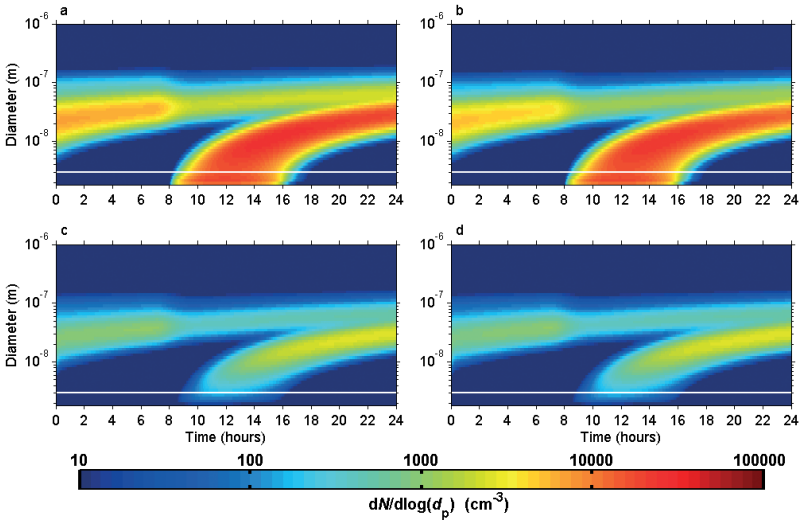

Fig. 1. Evolution of particle size distribution during the simulation case 1 for (**a**) total, (**b**) neutral, (**c**) negatively charged and (**d**) positively charged particles. Color indicates the particle number concentration ($dN/d\log d_p$) as a function of time and diameter. All particles were formed as neutral at 1.8 nm.

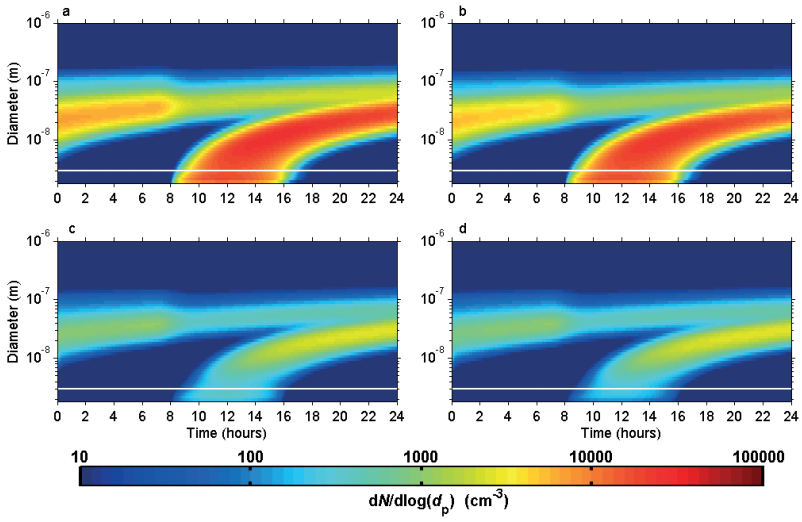

Fig. 2. Same as Fig. 1, except that the formation rate of neutral, negatively and positively charged particles were 85%, 10% and 5% of the total particle formation rate, respectively.

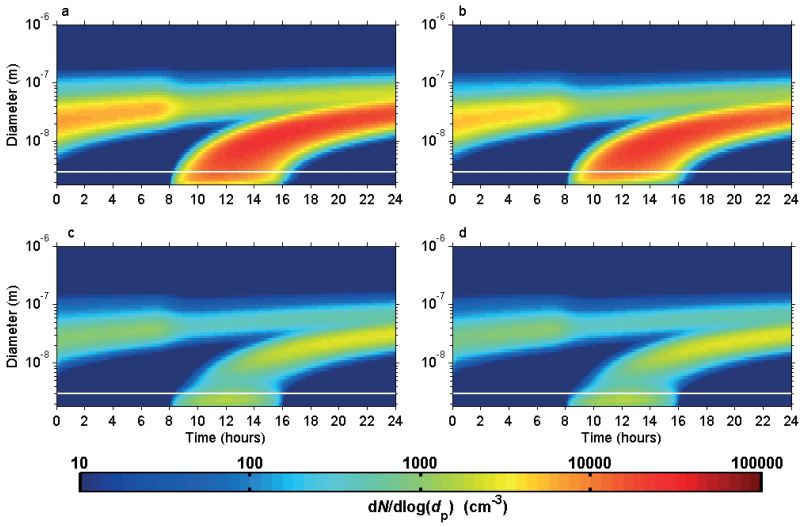

Fig. 3. Same as Fig. 1, except that half of the particles were formed negatively charged and the other half positively charged.

of purely ion-induced particle formation and enhanced condensation onto charged particles, which led to the rapid growth of freshly-formed particles. Most of the charged particles were, however, neutralized quite rapidly during their growth in case 3 (Fig. 3).

Particle charging state and evolution toward charge equilibrium

The charging state, S, is defined as:

$$S_{\pm}\left(d_{\mathrm{p}}\right)=\frac{f_{\pm}\left(d_{\mathrm{p}}\right)}{f_{\pm,\mathrm{eq}}\left(d_{\mathrm{p}}\right)}=\frac{N_{\pm}\left(d_{\mathrm{p}}\right)/N_{\mathrm{tot}}\left(d_{\mathrm{p}}\right)}{f_{\pm,\mathrm{eq}}\left(d_{\mathrm{p}}\right)}, \quad (6)$$

where $f_{\pm}$ is the fraction of positively or negatively charged particles, $f_{\pm,\mathrm{eq}}$ is the corresponding fraction in charge equilibrium, $N_{\pm}$ is the concentration of positively or negatively charged particles and N_{tot} is the total particle concentration. The charging state is a useful indicator that describes the relative importance of ion-induced and neutral nucleation mechanisms (Iida *et al*. 2006, Vana *et al*. 2006, Laakso *et al*. 2007a, Gagné *et al*. 2008). Based on a number of simplifying assumptions, Kerminen *et al*. (2007) derived the following analytical formula for the behavior of the charging state as a function of particle diameter during a new particle formation event:

$$S\left(d_{\mathrm{p}}\right)=1-\frac{1}{Kd_{\mathrm{p}}}+\frac{1+\left(S_0-1\right)Kd_0}{Kd_{\mathrm{p}}}\exp\left[-K\left(d_{\mathrm{p}}-d_0\right)\right]. \quad (7)$$

Here, S_0 is the value of S at $d_{\mathrm{p}} = d_0$ and the parameter K is defined as

$$K=\frac{\alpha N_{\mathrm{C}}^{\pm}}{GR\left(d_{\mathrm{p}}\right)}, \quad (8)$$

where GR is the particle growth rate, $N_{\mathrm{C}}^{\pm}$ is the number concentration of positively or negatively charged clusters, and α is the ion-ion recombination coefficient.

In principle, the charging state S varies in time and parameter K varies both in time and as a function of particle size. When analyzing measurement data, only the median value of S calculated over the new particle formation event period for a small number of particle sizes can be determined (Laakso *et al*. 2007a, Gagné *et al*. 2008). Thus, only a single value for the parameter K is obtained for each event. The value of S as a function of particle diameter and the value of parameter K are nevertheless obtained for both negatively and positively charged particles. Here, we used a similar time-averaging approach when determining the values of S and K from simulations.

In order to calculate the charging state during a simulation in Ion-UHMA, the equilibrium charged fraction as a function of diameter for present conditions is needed. The equilibrium charged fraction is obtained by simulating the attachment of charged clusters on a dummy particle population until a steady state is reached.

The charging state from the model for each size section was obtained as a median value over the duration of the event in that section. The growth rate of the particles, needed to calculate the K parameters in Eq. 8, was obtained from the model. The growth rate output from the model is given as a function of time and particle diameter for each charge class. In order to get a single value to calculate the K parameters, the growth rate was averaged over the duration of the event and over the size range 1.8–10 nm, and a weighted average was taken over the charge classes. The concentrations of charged clusters were obtained as average values over the duration of the event. Simulated value of the charging state in the smallest size section (d_0 = 1.8 nm) was used as the reference value of charging state (S_0).

The charging states as a function of particle diameter was simulated for the cases 1, 2 and 3, introduced in the previous section (Fig. 4a). In case 1, the charging state was initially below unity but increased as the neutral particles were charged while growing to bigger sizes. In case 3, the initial charging state was very high because all new particles were initially charged, but the charging state decreased rapidly, as the particles were neutralized. In case 2, the formation rates of negative and positive particles were not the same, which is clearly observed in the charging states. The charging state of positive particles showed a slight increase just after 2-nm size before its decrease. This resulted from the enhanced condensational growth of charged par-

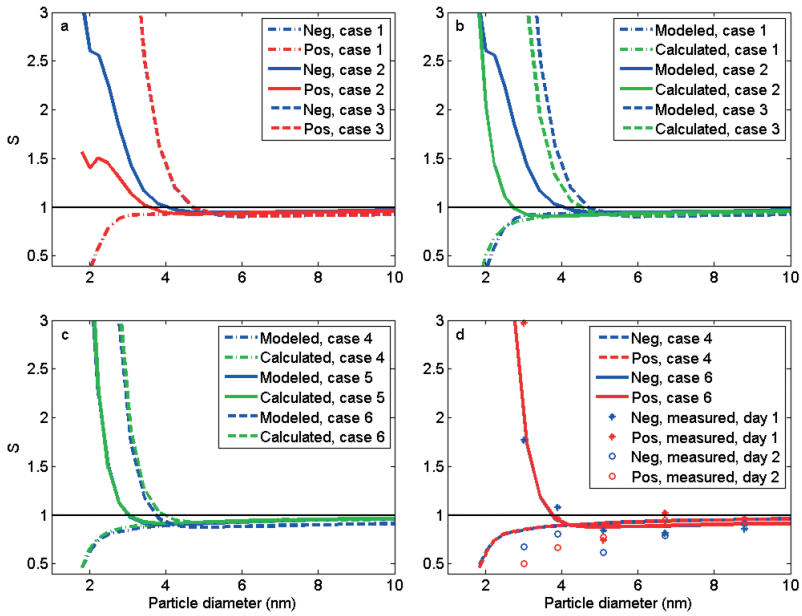

Fig. 4. Charging states (*S*) as a function of particle diameter from various methods. Blue and red indicate the charging state of negatively and positively charged particles, respectively. Green indicates the charging state of negatively charged particles calculated using Eq. 7. (**a**) simulated charging states of negatively and positively charged particles for cases 1, 2 and 3. (**b**) simulated and calculated charging states of negatively charged particles for cases 1, 2 and 3. (**c**) simulated and calculated charging states of negatively charged particles for cases 4, 5 and 6. (**d**) simulated charging states of cases 4 and 6, as well as measured charging states during 30 April and 4 April 2007 (asterisk and circle, respectively).

ticles, which increased the fraction of charged particle flux into bigger sizes. Such behavior was not observed for negative particles, for which the neutralization dominated over the increased flux of charged particles.

One of the assumptions made by Kerminen *et al*. (2007) in the derivation of Eq. 7 was that the particles grow at the same rate regardless of their charge. As a result, Eq. 7 is not able to capture the behavior of charging state of case 2 (Fig. 4b). In order to compare the charging state obtained from the model with that given by Eq. 7, three new simulations were conducted (cases 4, 5 and 6). Cases 4, 5 and 6 were exactly the same as cases 1, 2 and 3, correspondingly, except that enhanced condensation flux due to the presence of charges was not taken into account. Differences between calculated and simulated charging states for cases 4, 5 and 6 were very small and the behavior of the charging states as a function of diameter were qualitatively the same (Fig. 4c).

The charging state has been measured at the SMEAR II station (Laakso *et al*. 2007a, Gagné *et al*. 2008) and the diameter dependence of the measured charging states are similar to those seen in the simulations described above (Fig. 4d). The similarities in the behavior of the measured and simulated charging states (Fig. 4d) are only qualitative, as measured data was not used as input for the model. The measured days depicted in Fig. 4d were chosen so, that the initial charging state observed was either very low or high. In the case of initially high charging state, the measured charging states also dropped below unity before converging towards unity.

As a whole, the behavior of the charging state produced by the model is similar to that observed in the measurements, including the dipping below unity before converging towards unity. Also, the charging state obtained using Eq. 7 follows the simulated charging state very well, except in the case of heavily increased growth rate of charged particles, which could not be taken into account in the derivation of Eq. 7.

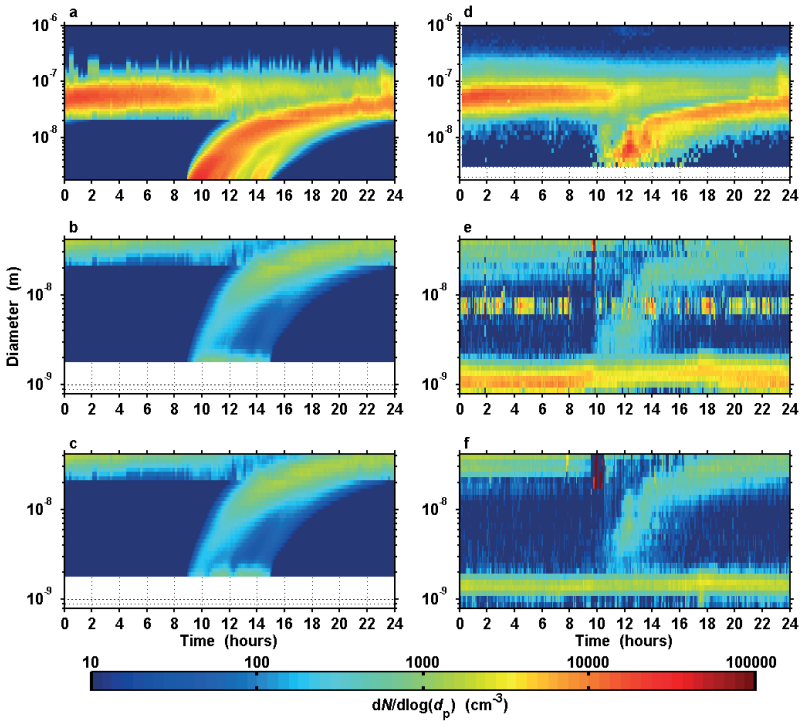

Fig. 5. Simulated (**a**, **b** and **c**) and measured (**d**, **e** and **f**) evolution of the particle number size distribution for 15 September 2006. The evolution is shown for total (**a** and **d**), negatively charged (**b** and **e**) and positively charged particles (**c** and **f**). Color indicates the particle number concentration ($dN/d\log d_p$) as a function of time and diameter. The new particle formation rate, the growth rate of the particles and concentrations of particles larger than 20 nm in diameter were taken from measurements and used as input for the simulation.

Application to measurement data

In order to test if Ion-UHMA is capable of reproducing the measured time evolution of the particle size distribution, a second set of simulations (set 2) was conducted. The simulations were conducted using 60 size sections and the simulated diameter range was from 1.8 nm to 1.0 μm. In these simulations, the following parameters were taken from measurements and used as inputs for the model: the particle size distribution from 20 to 1000 nm, concentrations and average mobilities of charged clusters, growth rate of particles and the formation rate of neutral and charged particles with diameter of 1.8 nm. For the details of the method used to determine the formation rate of particles *see* Manninen *et al*. (2009) and Kulmala *et al*. (2007). The particle size distribution from 20 to 1000 nm was updated every 10 minutes using the measured values. The measured growth rates were obtained as average values over the events for three diameter ranges (1.7–3 nm, 3–7 nm and 7–20 nm). The growth rates as a function of diameter were smoothed for the simulations in order to avoid step-like changes. The measurements were conducted at the SMEAR II station (*see* Hari and Kulmala 2005) in Hyytiälä, southern Finland, during the years 2006 and 2007 (Manninen *et al*. 2009, Nieminen *et al*. 2009).

Fourteen days were chosen with the restrictions that all the data listed above were available, that a new particle formation event was observed during the day, and that the measured air masses were sufficiently homogeneous. The last restriction is crucially important, as Ion-UHMA cannot simulate processes associated with changes in air mass transport patterns.

The model reproduced quite well the observed time evolution of the particle number size distribution for each of the simulated days. An example of such a day is depicted in Fig. 5

(the measured values used as input parameters for this example are diven in the Table 2). During the day the temperature rose from the minimum of 275 K to the maximum of 285 K between 06:00 and 15:00 and then decreased to 276 K between 15:00 and 20:00. The concentration of negative clusters rose steadily from minimum of ~600 cm^{-3} to a maximum of ~1100 cm^{-3} between 05:00 and 18:00 and the concentration of positive clusters was slightly higher than the concentration of negative ones. The total and charged particle concentrations were measured for the size ranges of 3–1000 nm and 0.8–40 nm, respectively (Fig. 5d, e and f). In the simulations, the concentrations of particles from 1.8 to 20 nm in diameter were simulated and the concentrations of larger particles were taken from the measurements. As a result, we may compare simulations and observations over the diameter range 3–20 nm for total particles (Fig. 5a and d) and over the diameter range 1.8–20 nm for negatively (Fig. 5b and e) and positively (Fig. 5c and f) charged particles. Furthermore, we may look at the boundary between simulation and measurement at the diameter of 20 nm (Fig. 5a, b and c). We may see that the evolution of particle concentrations were very similar and the concentrations at both sides of the boundary between simulation and measurement agreed well with each other.

In order to demonstrate potential ways to use Ion-UHMA in future studies, we conducted eight more simulations for each of the fourteen days mentioned above. In each simulation, we tried to reproduce the measured data of the particular day, with either the formation rate or the growth rate of particles multiplied by a factor of 2, 5, 0.5 or 0.2. The resulting evolution of the particle number size distribution was then visually compared with the measured one, to assess roughly whether a smaller or larger input growth rate or formation rate resulted in a better agreement between the simulation and measurements. Two examples of such simulations, associated with 15 September 2006, are shown in Fig. 6. In one of the examples the formation rate of the particles was multiplied by 0.2 (Fig. 6a, b and c) and in the other the particle growth rate was multiplied by 0.5 (Fig. 6d, e and f). Visual comparison of the evolutions of particle number size distributions shown in Figs. 5 and 6 indicates that in this case, the agreement between the measured and simulated evolutions of particle number size distributions is worse, if the formation or growth rate of the particles in the model is multiplied by 0.2 or 0.5, respectively.

For one of the days, the comparison was not reasonable due to significant differences in the diameter dependence of particle number concentration. For the remaining 13 days, the best agreement between measurements and simulation was usually obtained by multiplying the particle growth rate by a factor of 1 or 2. Factors above unity would suggest that the measured growth rate underestimates the real growth rate of the particles during the particular day. In the case of the particle formation rate, the best multiplier ranged from 0.2 to 5 between the different days. Since the simulated concentrations depend on both formation and growth rate of particles, in principle all the combinations of multipliers should be used to get full understanding on the best values. Also the comparison between measured and simulated evolutions of particle size distributions should be quantitative to get more precise results. This procedure was not done in this study, as our aim was only to show potential ways to use the model.

Table 2. Parameter values measured during 15 September 2006 and used as input in the model. The given values are averaged over the day, except for the growth and formation rates of the particles, which are averaged over the event.

Parameter	Value
Concentration of negative clusters	874 cm^{-3}
Concentration of positive clusters	947 cm^{-3}
Mobility of negative clusters	0.15×10^{-3}
Mobility of positive clusters	0.14×10^{-3}
Growth rate of 1.7–3.0 nm particles	2.21 nm h^{-1}
Growth rate of 3.0–7.0 nm particles	2.99 nm h^{-1}
Growth rate of 7.0–20.0 nm particles	4.02 nm h^{-1}
Total formation rate of particles	1.1 cm^{-3} s^{-1}
Formation rate of negative particles	0.12 cm^{-3} s^{-1}
Formation rate of positive particles	0.10 cm^{-3} s^{-1}
Temperature	279 K

Summary and conclusions

Here, we have introduced a new aerosol dynami-

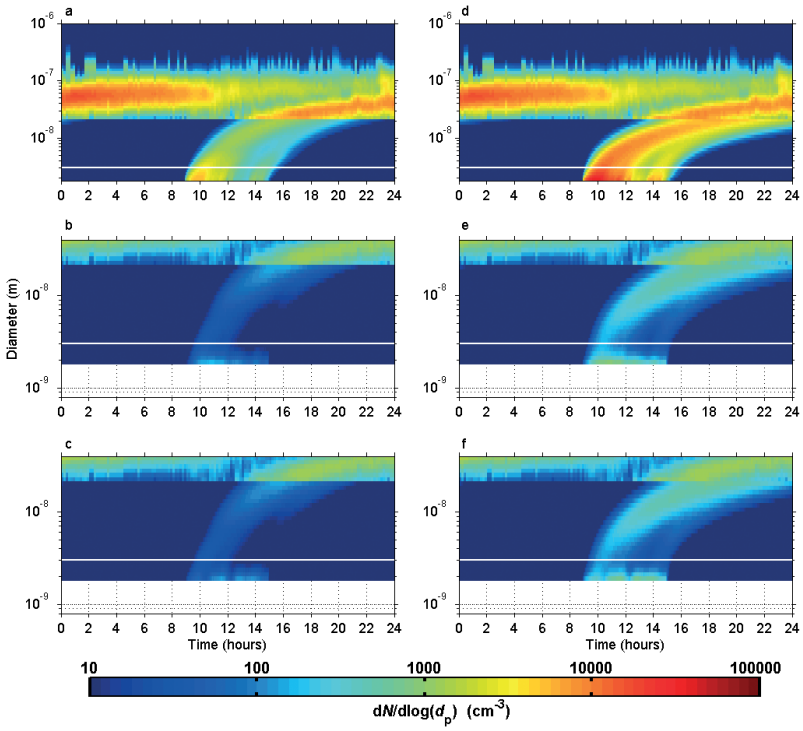

Fig. 6. Two simulated evolutions of the particle number size distribution for 15 September 2006. The evolution is shown for total (**a** and **d**), negatively charged (**b** and **e**) and positively charged (**c** and **f**) particles. Color indicates the particle number concentration ($dN/d\log d_p$) as a function of time and diameter. In the simulation shown in **a**, **b** and **c**, the measured formation rate of the particles used as input in the model was multiplied by a factor of 0.2; and in the simulation shown in **d**, **e** and **f**, the measured growth rate of the particles used as input in the model was multiplied by a factor of 0.5.

cal box model, Ion-UHMA, and tested its overall performance. The Ion-UHMA simulates the basic aerosol dynamical processes over the particle diameter range < 2 nm to 1000 nm using a sectional representation of the aerosol number size distribution. In each size section, three particle types are considered: neutral particles and particles containing a single positive or negative charge. Formation rates of new aerosol particle via nucleation are treated as a model input, which makes it possible to use measured new-particle formation rate data or, alternatively, to couple Ion-UHMA with any nucleation model. The Ion-UHMA model includes also pools for molecular clusters, making it possible to simulate the ion-ion recombination and ion-aerosol attachment processes.

With a few illustrative examples, we demonstrated that the Ion-UHMA model is capable of simulating the evolution of charged and neutral (total) particle populations during atmospheric nucleation events, as seen from observations. We showed further that the charging state of freshly-nucleated particles evolves toward charge equilibrium in line with our previously-derived analytical, yet approximate, formulae. This latter finding is crucial for determining the contribution of ion-induced nucleation to the overall new-particle formation rate using atmospheric measurement data.

Ion-UHMA could be used for several possible applications in the future. By combining Ion-UHMA simulations with ion spectrometer and ion-DMPS data from various locations, we should be able to get new insight into the very early steps of atmospheric new-particle formation. Especially, this might help us to resolve the continuing debate on the role of ions in atmospheric nucleation (e.g. Iida *et al*. 2006, Gagné *et al*. 2008, Kazil *et al*. 2008, Yu and Turco 2008).

The Ion-UHMA model can also be used to estimate how sensitive the dynamics of sub-5 nm particle populations are to different quantities, including measurement uncertainties. A concrete application in this regard would be to find out how reliably particle growth rates can be determined from current ion spectrometer measurements. Such information would be of high value for people analyzing the statistics of atmospheric nucleation events, as well as for people inserting nucleation parameterizations (*see* Kerminen *et al*. 2004, Mogdil *et al*. 2005, Kazil and Lovejoy 2007, Lehtinen *et al*. 2007) into large-scale atmospheric modeling systems.

Acknowledgements: This work has been supported by European Commission (6th Framework program project EUCAARI, Contract no. 036833-2), by the Academy of Finland Centre of Excellence program (project nos. 211483, 211484 and 1118615) and by Vilho, Yrjö and Kalle Vaisala Foundation.

References

Allan J.D., Alfarra M.R., Bower K.N., Coe H., Jayne J.T., Worsnop D.R., Aalto P.P., Kulmala M., Hyötyläinen T., Cavalli F. & Laaksonen A. 2006. Size and composition measurements of background aerosol and new particle growth in a Finnish forest during QUEST 2 using an Aerodyne Aerosol Mass Spectrometer. *Atmos. Chem. Phys*. 6: 315–327.

Anttila T., Kerminen V.-M., Kulmala M., Laaksonen A. & O'Dowd C.D. 2004. Modelling the formation of organic particles in the atmosphere. *Atmos. Chem. Phys*. 4: 1071–1083.

Arnold F. 1980. Multi-ion complexes in the stratosphere — implications for trace gases and aerosols. *Nature* 284: 610–611.

Asmi E., Sipilä M., Manninen H.E., Vanhanen J., Lehtipalo K, Gagne S., Neitola K., Mirme A., Mirme S., Tamm E., Uin J., Komsaare K., Attoui M. & Kulmala M. 2009. Results of first air ion spectrometer calibration and intercomparison workshop. *Atmos. Chem. Phys*. 9: 141–154.

Clement C.F., Kulmala M. & Vesala T. 1996. Theoretical considerations of sticking probability. *J. Aerosol. Sci*. 27: 869–882.

Davidovits P., Kolb C.E., Williams L.R., Jayne J.T. & Worsnop D.R. 2006. Mass accommodation and chemical reactions at gas-liquid interfaces. *Chem. Rev.* 106: 1323–1354.

Dal Maso M., Sogacheva L., Aalto P.P., Riipinen I., Komppula M., Tunved P., Korhonen L., Suur-Uski V., Hirsikko A., Kurtén T., Kerminen V.-M., Lihavainen H., Viisanen Y., Hansson H.-C. & Kulmala M. 2007. Aerosol size distribution measurements at four Nordic field stations: identification, analysis and trajectory analysis of new particle formation bursts. *Tellus* 59B. 350–361.

Fiedler V., Dal Maso M., Boy M., Aufmhoff H., Hoffmann T., Schuck T., Birmili W., Hanke M., Uecker J., Arnold F. & Kulmala M. 2005. The contribution of sulphuric acid to atmospheric particle formation and growth: a comparison between boundary layers in Northern and Central Europe. *Atmos. Chem. Phys*. 5: 1773–1785.

Fuchs N. 1964. *The mechanics of aerosols*. Dover, Mineola, N.Y.

Fuchs N.A. & Sutugin A.G. 1971. Highly dispersed aerosols. In: Hidy G.M. & Brock J.R. (eds.), *Topics in current aerosol research*, Pergamon Press, New York, pp. 1–60.

Gagné S., Laakso L., Petäjä T., Kerminen V.-M. & Kulmala M. 2008. Analysis of one year of Ion-DMPS data from the SMEAR II station, Finland. *Tellus* 60B: 318–329.

Guimbaud C., Arens F., Gutzwiller L., Gaggeler H.W. & Ammann M. 2002. Uptake of HNO_3 to deliquescent sea-salt particles: a study using the short-lived radioactive isotope tracer 13N. *Atmos. Chem. Phys*. 2: 249–257.

Hanson D. & Kosciuch E. 2003. The NH_3 mass accommodation coefficient for uptake onto sulfuric acid solutions. *J. Phys. Chem*. A. 107: 2199–2208.

Hari P. & Kulmala M. 2005. Station for Measuring Ecosystem-Atmosphere Relations (SMEAR II). *Boreal Env. Res*. 5: 315–322.

Hirsikko A., Laakso L., Hõrrak U., Aalto P.P., Kerminen V.-M. & Kulmala M. 2005. Annual and size dependent variation of growth rates and ion concentrations in boreal forest. *Boreal Env. Res*. 10: 357–369.

Hirsikko A., Bergman T., Laakso L., Dal Maso M., Riipinen I., Hõrrak U. & Kulmala M. 2007. Identification of the formation of intermediate ions measured in boreal forest. *Atmos. Chem. Phys*. 7: 201–210.

Hoppel W.A. & Frick G.M. 1986. Ion-aerosol attachment coefficients and the steady-state charge distribution on aerosols in a bipolar ion environment. *Aerosol Sci. Technol*. 5: 1–21.

Hoppel W.A. & Frock G.M. 1990. The nonequilibrium character of the aerosol charge distribution produced by neutralizers. *Aerosol Sci. Technol*. 12: 471–496.

Hoppel W.A., Frick G.M., Fitzgerald J.W. & Larsson R.E. 1994. Marine boundary layer measurements of new particle formation and the effects nonprecipitating clouds have on aerosol size distributions. *J. Geophys. Res*. 99: 14443–14459.

Hõrrak U., Salm J. & Tammet H. 2003. Diurnal variation in the concentration of air ions of different mobility classes in a rural area. *J. Geophys. Res*. 108(D20), 4653, doi:10.1029/2002JD003240.

Hõrrak U., Aalto P.P., Salm J., Komsaare K., Tammet H., Mäkelä J.M., Laakso L. & Kulmala M. 2008. Variation and balance of positive air ion concentrations in a boreal forest. *Atmos. Chem. Phys*. 8: 655–675.

Howard J., Wersborg B. & Williams G. 1973. Coagulation of carbon particles in premixed flames. *Faraday Symp. Chem. Soc*. 7: 109–119.

Iida K., Stolzenburg M., McMurry P., Dunn M.J., Smith J.N., Eisele F. & Keady P. 2006. Contribution of ion-induced nucleation to new particle formation: Methodology and its application to atmospheric observations

in Boulder, Colorado. *J. Geophys. Res.* 111, D23201, doi:10.1029/2006JD007167.

Jacobson M.Z. & Turco R.P. 1995. Simulating condensational growth, evaporation, and coagulation of aerosols using a combined moving and stationaty size grid. *Aerosol Sci. Technol.* 22: 73–92.

Junninen H., Hulkkonen M., Riipinen I., Nieminen T., Hirsikko A., Suni T., Boy M., Lee S.-H., Vana M., Tammet H., Kerminen V.-M. & Kulmala M. 2008. Observations on nocturnal growth of atmospheric clusters. *Tellus* 60B: 365–371.

Kazil J. & Lovejoy E.R. 2004. Tropospheric ionization and aerosol production: A model study. *J. Geophys. Res.* 109, D19206, doi:10.1029/2004JD004852.

Kazil J. & Lovejoy E.R. 2007. A semi-analytical method for calculating rates of new sulfate aerosol formation from the gas phase. *Atmos. Chem. Phys.* 7: 3447–3459.

Kazil J., Harrison R.G. & Lovejoy E.R. 2008. Troposheric new particle formation and the role of ions. *Space Sci. Rev.* 137: 241–255.

Kerminen V.-M., Anttila T., Lehtinen K.E.J. & Kulmala M. 2004. Parametrization for atmospheric new-particle formation: application to a system involving sulfuric acid and condensable water-soluble organic vapors. *Aerosol Sci. Technol.* 38: 1001–1008.

Kerminen V.-M., Lihavainen H., Komppula M., Viisanen Y. & Kulmala M. 2005. Direct observational evidence linking atmospheric aerosol formation and cloud droplet activation. *Geophys. Res. Lett.* 32, L14803, doi:10.1029/2005GL023130.

Kerminen V.-M., Anttila T., Petäjä T., Laakso L., Gagné S., Lehtinen K.E.J. & Kulmala M. 2007. Charging state of the atmospheric nucleation mode: implications for separating neutral and ion-induced nucleation. *J. Geophys. Res.* 112: D21205, doi:10.1029/2007JD008649.

Komppula M., Vana M., Kerminen V.-M., Lihavainen H., Viisanen Y., Hõrrak U., Komsaare K., Tamm E., Hirsikko A., Laakso L. & Kulmala M. 2007. Size distributions of atmospheric ions in the Baltic Sea region. *Boreal Env. Res.* 12: 323–336.

Korhonen H., Lehtinen K.E.J. & Kulmala M. 2004. Multicomponent aerosol dynamics model UHMA: model development and validation. *Atmos. Chem. Phys.* 4: 757–771.

Kuang C., McMurry P.H., McCormick A.V. & Eisele F.L. 2008. Dependence of nucleation rates on sulfuric acid vapor concentration in diverse atmospheric locations. *J. Geophys. Res.* 113, D10209, doi:10.1029/2007JD009253.

Kulmala M. & Wagner P.E. 2001. Mass accommodation and uptake coefficients — a quantitative comparison. *J. Aerosol Sci.* 32: 833–841.

Kulmala M. & Tammet H. 2007. Finnish–Estonian air ion and aerosol workshops. *Boreal Env. Res.* 12: 237–245.

Kulmala M. & Kerminen V.-M. 2008. On the formation and growth of atmospheric nanoparticles. *Atmos. Res.* 90: 132–150.

Kulmala M., Lehtinen K.E.J. & Laaksonen A. 2006. Cluster activation theory as an explanation of the linear dependence between formation rate of 3 nm particles and sulphuric acid concentration. *Atmos. Chem. and Phys.* 6: 787–793.

Kulmala M., Kerminen V.-M., Anttila T., Laaksonen A. & O'Dowd C. 2004a. Organic aerosol formation via sulphate cluster activation. *J. Geophys. Res.* 109: D04205, doi:10.1029/2003JD003961.

Kulmala M., Vehkamäki H., Petäjä T., Dal Maso M., Lauri A., Kerminen V.-M., Birmili W. & McMurry P.H. 2004b. Formation and growth rates of ultrafine atmospheric particles: a review of observations. *J. Aerosol Sci.* 35: 143–176.

Kulmala M., Laakso L., Lehtinen K.E.J., Riipinen I., Dal Maso M., Anttila T., Kerminen V.-M., Horrak U., Vana M. & Tammet H. 2004c. Initial steps of aerosol growth. *Atmos. Chem. Phys.* 4: 2553–2560.

Kulmala M., Riipinen I., Sipilä M., Manninen H.E., Petäjä T., Junninen H., Dal Maso M., Mordas G., Mirme A., Vana M., Hirsikko A., Laakso L., Harrison R. M., Hanson I., Leung C., Lehtinen K.E.J. & Kerminen V.-M. 2007. Towards direct measurement of atmospheric nucleation. *Science* 318: 89–92.

Laakso L., Mäkelä J.M., Pirjola L. & Kulmala M. 2002. Model studies on ion-induced nucleation in the atmosphere. *J. Geophys. Res.* 107(D20), 4427, doi:10.1029/2002JD002140.

Laakso L., Gagné S., Petäjä T., Hirsikko A., Aalto P.P., Kulmala M. & Kerminen V.-M. 2007a. Detecting charging state of ultrafine particles: instrumental development and ambient measurements. *Atmos. Chem. Phys.* 7: 1333–1345.

Laakso L., Grönholm T., Kulmala L., Haapanala S., Hirsikko A., Lovejoy E.R., Kazil J., Kurten T., Boy M., Nilsson E.D., Sogachev A., Riipinen I., Stratmann F. & Kulmala M. 2007b. Hot-air balloon as a platform for boundary layer profile measurements during particle formation. *Boreal Env. Res.* 12: 279–294.

Laaksonen A., Hamed A., Joutsensaari J., Hiltunen L., Cavalli F., Junkermann W., Asmi A., Fuzzi S. & Facchini M.C. 2005. Cloud condensation nucleus production from nucleation events at a highly polluted region. *Geophys. Res. Lett.* 32, L06812, doi:10.1029/2004GL022092.

Lehtinen K.E.J. & Kulmala M. 2003. A model for particle formation and growth in the atmosphere with molecular resolution in size. *Atmos. Chem. Phys.* 2: 251–257.

Lehtinen K.E.J., Dal Maso M., Kulmala M. & Kerminen V.-M. 2007. Estimating nucleation rates from apparent particle formation rates and vice-versa: revised formulation of the Kerminen–Kulmala equation. *J. Aerosol Sci.* 38: 988–994.

Lovejoy E.R., Curtius J. & Froyd K.D. 2004. Atmospheric ion-induced nucleation of sulfuric acid and water. *J. Geophys. Res.* 109, D08204, doi:10.1029/2003JD004460.

Lushnikov A.A. & Kulmala M. 2004. Charging of aerosol particles in the near free-molecule regime. *Eur. Phys. J.* D29: 345–355.

Makkonen R., Asmi A., Korhonen H., Kokkola H., Järvenoja S., Räisänen P., Lehtinen K.E.J., Laaksonen A., Kerminen V.-M., Järvinen H., Lohmann U., Bennartz R., Feichter J. & Kulmala M. 2009. Sensitivity of aerosol concentrations and cloud properties to nucleation and secondary organic distribution in ECHAM5-

HAM global circulation model. *Atmos. Chem. Phys.* 9: 1747–1766.

Manninen H.E., Nieminen T., Riipinen I., Yli-Juuti T., Gagné S., Petäjä T., Asmi E., Aalto P.P., Kerminen V.-M. & Kulmala M. 2009. Charged and total particle formation and growth rates during EUCAARI 2007 campaign in Hyytiälä. *Atmos. Chem. Phys.* 9: 4077–4089.

Mirme A., Tamm E., Mordas G., Vana M., Uin J., Mirme S., Bernotas T., Laakso L., Hirsikko A. & Kulmala M. 2007. A wide-range multi-channel Air Ion Spectrometer. *Boreal Env. Res.* 12: 247–264.

Mick H.J., Hospital A. & Roth P. 1991. Computer simulation of sooth particle coagulation in low pressure flames. *J. Aerosol Sci.* 22: 831–841.

Mogdil M.S., Kumar S., Tripathi S.N. & Lovejoy E.R. 2005. A parameterization of ion-induced nucleation of sulphuric acid and water for atmospheric conditions. *J. Geophys. Res.* 110, D19205, doi:10.1029/2004JD005475.

Morita A. 2003. Molecular dynamics study of mass accommodation of methanol at liquid-vapor interfaces of methanol/water binary solutions of water concentrations. *Chem. Phys. Lett.* 375: 1–8.

Napari I., Noppel M., Vehkamäki H. & Kulmala M. 2002. An improved model for ternary nucleation of sulfuric acid–ammonia–water. *J. Chem. Phys.* 116: 4221–4227.

Nieminen T., Manninen H.E., Sihto S.-L., Yli-Juuti T., Mauldin R.L.III, Petäjä T., Riipinen I., Kerminen V.-M. & Kulmala M. 2009. Connection of sulphuric acid to atmospheric nucleation in boreal forest. *Environ. Sci. Technol.* 43. [In press].

O'Dowd C.D., Aalto P., Hämeri K., Kulmala M. & Hoffmann T. 2002. Atmospheric particles from organic vapours. *Nature* 416: 497–498.

Pierce J.R. & Adams P.J. 2007. Efficiency of cloud condensation nuclei formation from ultrafine particles. *Atmos. Chem. Phys.* 7: 1367–1379.

Pierce J.R. & Adams P.J. 2009. Uncertainty in global CCN concentrations from uncertain aerosol nucleation and primary emission rates. *Atmos. Chem. Phys.* 9: 1339–1356.

Rannik Ü., Aalto P., Keronen P., Vesala T. & Kulmala M. 2003. Interpretation of aerosol particle fluxes over a pine forest. Dry deposition and random errors. *J. Geophys. Res.* 108(D17), 4544, doi: 10.1029/2003JD003542.

Riipinen I., Sihto S.-L., Kulmala M., Arnold F., Dal Maso M., Birmili W., Saarnio K., Teinilä K., Kerminen V.-M., Laaksonen A. & Lehtinen K.E.J. 2007. Connections between atmospheric sulphuric acid and new particle formation during QUEST III–IV campaigns in Heidelberg and Hyytiälä. *Atmos. Chem. Phys.* 7: 1899–1914.

Sihto S.-L., Kulmala M., Kerminen V.-M., Dal Maso M., Petäjä T., Riipinen I., Korhonen H., Arnold F., Janson R., Boy M., Laaksonen A. & Lehtinen K.E.J. 2006. Atmospheric sulphuric acid and aerosol formation: implications from atmospheric measurements for nucleation and early growth mechanisms. *Atmos. Chem. Phys.* 6: 4079–4091.

Siingh D., Pant V. & Kamra A.K. 2007. Measurements of positive ions and air–Earth current density at Maitri, Antarctica. *J. Geophys. Res.* 112, D13212, doi:10.1029/2006JD008101.

Smith J.N., Dunn M.J., VanReken T.M., Iida K., Stolzenburg M.R., McMurry P.H. & Huey L.G. 2008. Chemical composition of atmospheric nanoparticles formed from nucleation in Tecamac, Mexico: evidence for an important role for organic species in nanoparticle growth. *Geophys. Res. Lett.* 35, L05808, doi:10.1029/2007GL032523.

Sorokin A., Arnold F. & Wiedner D. 2006. Formation and growth of sulfuric acid–water cluster ions: Experiments, modeling, and implications for ion-induced aerosol formation. *Atmos. Environ.* 40: 2030–2045.

Spracklen D.V., Carslaw K.S., Kulmala M., Kerminen V.-M., Mann G.W. & Sihto S.-L. 2006. The contribution of boundary layer nucleation events to total particle concentrations on regional and global scales. *Atmos. Chem. Phys.* 6: 5631–5648.

Spracklen D.V., Carslaw K.S., Kulmala M., Kerminen V.-M., Sihto S.-L., Riipinen I., Merikanto J., Mann G.W., Chipperfield M.P., Wiedensohler A., Birmili W. & Lihavainen H. 2008. Contribution of particle formation to global cloud condensation nuclei concentrations. *Geophys. Res. Lett.* 35, L06808, doi:10.1029/2007GL033038.

Suni T., Kulmala M., Hirsikko A., Bergman T., Laakso L., Aalto P.P., Leuning R., Cleugh H., Zegelin S., Hughes D., van Gorsel E., Kitchen M., Vana M., Hõrrak U., Mirme S., Mirme A., Sevanto S., Twining J. & Tadros C. 2008. Formation and characteristics of ions and charged particles in a native Australian eucalypt forest. *Atmos. Chem. Phys.* 8: 129–139.

Tammet H. 2006. Continuous scanning of the mobility and size distribution of charged clusters and nanometer particles in atmospheric air and the Balanced Scanning Mobility Analyzer BSMA. *Atmos. Res.* 82: 523–535.

Tammet H. & Kulmala M. 2005. Simulation tool for atmospheric aerosol nucleation bursts. *J. Aerosol Sci.* 36: 173–196.

Tammet H., Kimmel V. & Israelsson S. 2001. Effect of atmospheric electricity on dry deposition of airborne particles from atmosphere. *Atmos. Environ.* 35: 3423–3419.

Tunved P., Hansson H.-C., Kerminen V.-M., Ström J., Dal Maso M., Lihavainen H., Viisanen Y., Aalto P.P., Komppula M. & Kulmala M. 2006. High natural aerosol loading over boreal forests. *Science* 312: 261–263.

Vana M., Kulmala M., Dal Maso M., Hõrrak U. & Tamm E. 2004. Comparative study of nucleation mode aerosol particles and intermediate air ion formation events at three sites. *J. Geophys. Res.* 109, D17201, doi:10.1029/2003JD004413.

Vana M., Tamm E., Hõrrak U., Mirme A., Tammet H., Laakso L., Aalto P.P. & Kulmala M. 2006. Charging state of atmospheric nanoparticles during the nucleation burst events. *Atmos. Res.* 82: 536–546.

Vartiainen E., Kulmala M., Ehn M., Hirsikko A. Junninen H., Petäjä T., Sogacheva L., Kuokka S., Hillamo R., Skorokhod A., Belikov I., Elansky N. & Kerminen V.-M. 2007. Ion and particle number concentrations and size distributions along the Trans-Siberian railroad. *Boreal Env. Res.* 12: 375–396.

Voigtländer J., Stratmann F., Niedermeier D., Wex H. & Kiselev A. 2007. Mass accommodation coefficient of water: a combined computational fluid dynamics and experimental data analysis. *J. Geophys. Res.* 112, D20208, doi:10.1029/2007JD008604.

Wang M. & Penner J.E. 2009. Aerosol indirect forcing in a global model with particle nucleation. *Atmos. Chem. Phys.* 9: 239–260.

Weber R.J., Marti J.J., McMurry P.H., Eisele F.L., Tanner D.J. & Jefferson A. 1996. Measured atmospheric new particle formation rates: implications for nucleation mechanisms. *Chem. Eng. Comm.* 151: 53–64.

Winkler P., Vrtala A., Wagner P., Kulmala M., Lehtinen K.E.J. & Vesala T. 2004. Mass and thermal accommodation during gas-liquid condensation of water. *Phys. Rev. Lett.* 93, doi:10.1103/PhysRevLett.93.075710.

Winkler P., Steiner G., Vrtala A., Vehkamäki H., Noppel M., Lehtinen K.E.J., Reischl G.P., Wagner P.E. & Kulmala M. 2008. Heterogeneous nucleation experiments bridging the scale from molecular ion clusters to nanoparticles. *Science* 319: 1374–1377.

Worsnop D.R., Shi Q., Jayne J.T., Kolb C.E., Swartz E. & Davidovits P. 2001. Gas-phase diffusion in droplet train measurements of uptake coefficients. *J. Aerosol Sci.* 32: 877–891.

Yu F. 2006. From molecular clusters to nanoparticles: second-generation ion-meditated nucleation model. *Atmos. Chem. Phys.* 6: 5193–5211.

Yu F. & Turco R.P. 2001. From molecular clusters to nanoparticles: Role of ambient ionization in tropospheric aerosol formation. *J. Geophys. Res.* 106: 4797–4814.

Yu F. & Turco R.P. 2008. Case studies of particle formation events observed in boreal forests: implications for nucleation mechanisms. *Atmos. Chem. Phys.* 8: 6085–6102.